Electronic Supplementary Information

Two-dimensional metal-organic frameworks $Mo_3(C_2O)_{12}$ as promising single-atom catalysts for selective nitrogen-to-ammonia

Zhen Feng,[*a, b] Zelin Yang,[a] Xiaowen Meng,[a] Fachuang Li,[a] Zhanyong Guo,[a] Shu Zheng,[a] Guang Su,[a] Yaqiang Ma,[b] [1]Yanan Tang,[*c] and Xianqi Dai [*b]

.

[a] School of Materials Science and Engineering, Henan Institute of Technology, Xinxiang, Henan 453000, China. E-mail: fengzhen27@126.com.

[b] School of Physics, Henan Normal University, Xinxiang, Henan 453007, China. E-mail: xqdai@htu.edu.cn.

[c] College of Physics and Electronic Engineering, Zhengzhou Normal University, Zhengzhou 450044, China. E-mail: yntang2010@163.com.

†Electronic Supplementary Information (ESI) available: See DOI:10.1039/ x0xx00000x

Note S1 Electrochemical reaction computations

The free-energy change (ΔG) for each fundamental step was evaluated by computing $\Delta G = \Delta E + \Delta E_{ZPE} - T\Delta S + \Delta G_U + \Delta G_{pH} + \Delta G_{field}$ [1], where ΔE is the electronic energy difference, ΔE_{ZPE} is the zero-point energy (*ZPE*), T is 298.15 K, and ΔS is the difference in entropy. $\Delta G_{\mathrm{U}}=eU$, where U is the electrode potential, and e is the electron transfer. $\Delta G_{\mathrm{pH}} = k_{\mathrm{B}}T \times \ln 10 \times pH$, where k_{B} is the Boltzmann constant, and pH=0 in this study. $\Delta G_{\mathrm{field}}$ is neglected. The entropies and vibrational frequencies of the gas species are taken from the NIST database [2]. The calculated ΔE_{ZPE} and $T\Delta S$ of free molecules and reaction intermediates are summarized in **Table S1**.

Supplementary Figures

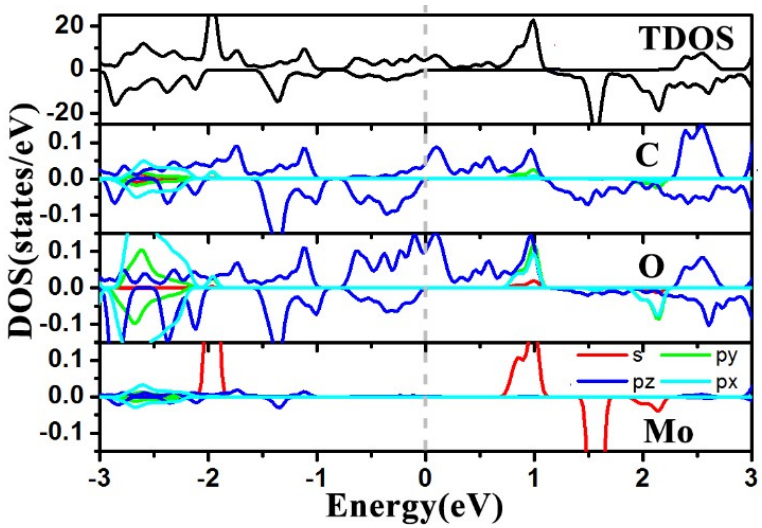

Fig. S1. TDOS of Mo-O MOF and PDOS of C, O, Mo element in Mo-O MOF monolayer. The Fermi level is set to 0 eV.

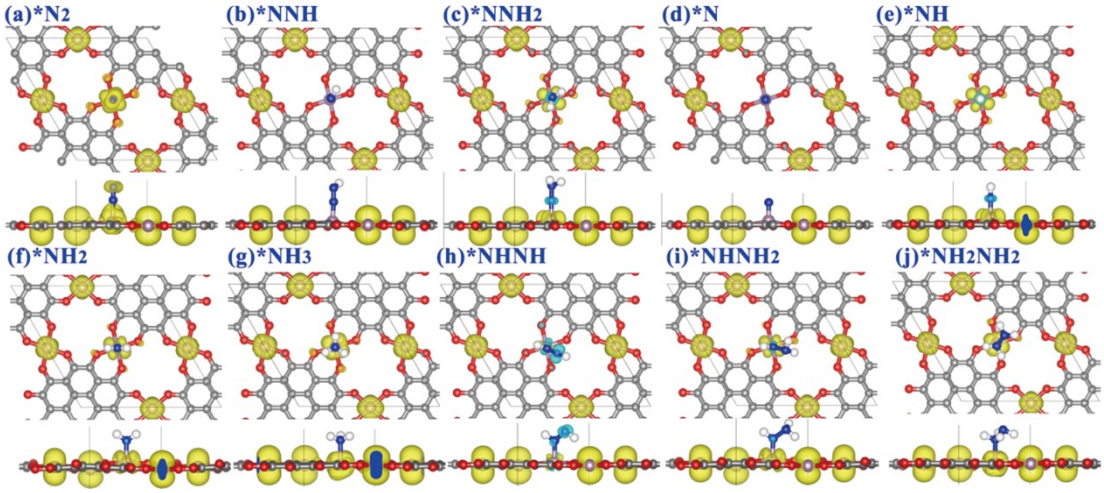

Fig. S2. The spin density of NRR species on Mo-O MOF monolayer. The isosurface value is 0.005 e $Å^{-3}$.

Supplementary Tables

Table S1 Zero-point energy corrections (ΔE_{ZPE}) and entropic contributions (at 298.15 K) to the free energies of the adsorption species and molecules on TM-O MOF monolayer estimated from the vibrational frequencies, * denotes TM-O MOF.

Species	ΔE_{ZPE}	$T\Delta S$
$*N_2$	0.19	0.16
*NNH	0.45	0.15
$*NNH_2$	0.83	0.17
*NHNH	0.81	0.14
$*NHNH_2$	1.13	0.17
$*NH_2NH_2$	1.42	0.20
*N	0.09	0.04
*NH	0.34	0.09
$*NH_2$	0.64	0.14
$*NH_3$	1.01	0.11
*H	0.16	0.02
N_2	0.15	0.59
H_2	0.27	0.41
NH_3	0.58	0.56

Table S2 Calculated lattice constants (l_a) for different TM-O MOF monolayers.

Materials	Sc-	Ti-	V-	Cr-	Mn-	Fe-	Co-	Ni-	Cu-	Zn-
l_a (Å)	12.83	12.58	12.48	12.50	12.39	12.31	12.26	12.26	12.48	12.63
Materials	Y	Zr	Nb	**Mo**	Tc	Ru	Rh	Pd	Ag	Cd
l_a (Å)	13.18	12.87	12.73	**12.67**	-	12.56	12.54	12.55	13.04	13.14
Materials	La	Hf	Ta	W	Re	Os	Ir	Pt	Au	Hg
l_a (Å)	-	12.83	12.70	12.59	12.65	12.55	12.52	12.52	12.53	-

Table S3 Calculated adsorption free energy [$\Delta G(*N_2)$] of N_2, the distance between TM atom and N_2 molecule (D_{TM-N}), and N-N bond length (L_{N-N}) for $*N_2$/TM-O MOF systems.

Materials		Sc-	Ti-	V-	Cr-	Mn-	Fe-	Co-	Ni-	Cu-	Zn-
$\Delta G(*N_2)$ (eV)	End	-0.21	-0.94	0.31	0.31	0.30	0.33	0.35	0.35	0.31	0.25
	Side	-	-	0.36	0.31	0.29	0.28	0.35	0.35	0.31	0.25
D_{TM-N} (Å)	End	1.83	2.10	2.74	2.73	2.60	3.28	3.22	3.24	3.13	2.73
	Side	-	-	3.60	2.71	2.58	3.19	3.18	3.24	3.31	2.70
L_{N-N} (Å)	End	1.14	1.12	1.11	1.11	1.11	1.11	1.11	1.11	1.11	1.11
	Side	-	-	1.11	1.11	1.11	1.11	1.11	1.11	1.11	1.11
Materials		Y	Zr	Nb	**Mo**	Tc	Ru	Rh	Pd	Ag	Cd
$\Delta G(*N_2)$ (eV)	End	-0.15	-0.99	0.33	**-0.05**	-	0.14	0.36	0.35	0.28	0.25
	Side	-	-	0.34	**0.50**	-	0.36	0.36	0.35	0.25	0.25
D_{TM-N} (Å)	End	2.51	2.25	2.77	**1.91**	-	3.41	3.32	3.78	3.09	2.89
	Side	-	-	2.78	**2.07**	-	3.41	3.86	3.33	3.42	2.85
L_{N-N} (Å)	End	1.12	1.12	1.11	**1.15**	-	1.11	1.11	1.11	1.11	1.11
	Side	-	-	1.11	**1.19**	-	1.11	1.11	1.11	1.11	1.11
Materials		La	Hf	Ta	W	Re	Os	Ir	Pt	Au	Hg
$\Delta G(*N_2)$ (eV)	End	-	-0.98	0.38	0.32	0.33	0.33	0.36	0.35	0.22	-
	Side	-	-0.83	0.34	0.38	0.67	0.34	0.36	0.35	0.22	-
D_{TM-N} (Å)	End	-	2.18	3.64	3.30	2.72	3.61	3.51	3.49	3.35	-
	Side	-	2.34	4.05	3.73	2.94	3.58	3.52	3.45	3.62	-
L_{N-N} (Å)	End	-	1.12	1.11	1.11	1.11	1.11	1.11	1.11	1.11	-
	Side	-	1.15	1.11	1.11	1.11	1.11	1.11	1.11	1.11	-

Table S4 Calculated adsorption free energy [$\Delta G(*NNH)$] of NNH, the distance between TM atom and N_2 molecule (D_{TM-N}), and N-N bond length (L_{N-N}) for NNH/TM-O MOF systems.

Materials		Sc-	Ti-	Y-	Zr-	**Mo-**	Hf-
$\Delta G(*NNH)$ (eV)	End	1.71	1.49	1.74	1.39	**0.27**	0.98
	Side	-	-	-	-	**-**	0.59
D_{TM-N} (Å)	End	2.11	1.87	2.26	2.03	**1.75**	2.01
	Side	-	-	-	-	**-**	2.15
L_{N-N} (Å)	End	1.19	1.21	1.20	1.22	**1.24**	1.22
	Side	-	-	-	-	**-**	1.24

Table S5 Calculated N-N bond length (L_{N-N}, Å), the distance between TM atom and adsorbed intermediates (D_{TM-N}, Å). Charge analysis of Mo atoms (Q Mo, e), O atoms (Q O_4, e), graphene linkers (Q graphene, e) and adsorbed intermediates (Q ads, e) for the adsorbed systems. The total magnetic moment $M_T(\mu_B)$ of the adsorbed systems. The positive and negative numbers represent electrons gained and lost, respectively.

Systems	L_{N-N} (Å)	D_{Mo-N} (Å)	Q_{Mo} (e)	QO_4 (e)	$Q_{graphene}$ (e)	Q_{ads} (e)	$M_T(\mu_B)$
Mo-O MOF	-	-	-2.02	+4.68	-2.66	-	6.00
N_2/Mo-O MOF	1.15	1.91	-2.19	+6.18	-4.35	+0.36	5.68
NNH/Mo-O MOF	1.24	1.75	-2.35	+6.14	-4.30	+0.51	3.41
NNH_2/Mo-O MOF	1.33	1.72	-2.04	+6.24	-4.66	+0.46	4.00
N...NH_3/Mo-O MOF	3.32	-	-	-	-	-	3.00
N/Mo-O MOF	-	1.64	-2.44	+6.22	-4.54	+0.76	3.00
NH/Mo-O MOF	-	1.70	-2.34	+6.28	-4.51	+0.57	4.00
NH_2/Mo-O MOF	-	1.90	-2.29	+6.11	-4.14	+0.32	5.00
NH_3/Mo-O MOF	-	2.17	-2.26	+2.87	-0.46	-0.15	6.00
NHNH/Mo-O MOF	1.29	1.93	-2.24	+6.09	-4.16	+0.31	3.63
$NHNH_2$/Mo-O MOF	1.41	1.89	-2.32	+4.54	-2.46	+0.24	5.00
NH_2NH_2/Mo-O MOF	1.46	2.14	-2.13	+4.60	-2.29	-0.18	6.00
NH_2...NH_3/Mo-O MOF	3.63	-	-	-	-	-	5.00

Table S6 The calculated limiting potentials (U_L in V) and PLS for the different catalysts that have been synthesized or designed recently.

Systems	Pathway	PLS	U_L (V)	References
Mo-O MOF	**Distal**	***NH_2+H^++e^-→*NH_3**	**-0.36**	**The present work**
V@GDY	Distal/ Alternating	*N_2+H^++e^-→*NNH	-0.67	Feng et al. 2020 [3]
Ru_1-N_3	Distal	*N_2+H^++e^-→*NNH	-0.73	Li et al. 2018[4]
Ru_1-N_4	Distal	*N_2+H^++e^-→*NNH	-0.77	Li et al. 2018[4]
Defect-rich MoS_2	Distal	*NH_2+H^++e^-→*NH_3	-0.60	Li et al. 2018[5]
MoS_2 with Mo edge	Distal	*N_2+H^++e^-→*NNH	-0.68	Zhang et al. 2018[6]
Mo_2C (111)	Distal	*N_2+H^++e^-→*NNH	-0.74	Ren et al. 2019[7]
Mo_2C (002)	Distal	*NH_2+H^++e^-→*NH_3	-0.92	Chen et al. 2018[8]
Ru(0001)	Distal	*N_2+H^++e^-→*NNH	-0.94	Skulason et al. 2012[9]
Co_2@GDY	Distal	*NH_2+H^++e^-→*NH_3	-0.43	Ma et al. 2019[10]
Nb_2O_5 (181)	Distal	*NNH_2+H^++e^-→*N+NH_3	-0.56	Han et al. 2018[11]
Ru_1@C_2N	Distal/ Alternating	*N_2+H^++e^-→*NNH	-0.96	Cao et al. 2018 [12]
Mo-embedded BN monolayer	Enzymatic	*NH_2+H^++e^-→*NH_3	-0.35	Zhao et al. 2017[13]
Mo@g-CN	Distal	*N_2+H^++e^-→*NNH	-0.39	Guo et al. 2020[14]
Mo^0/GDY	Alternating	*NHNH+H^++e^-→*$NHNH_2$	-0.71	Hui et al. 2019[15]
CrN_2B_2	Enzymatic	*N_2+H^++e^-→*NNH	-0.33	Fang et al. 2021[16]
NiCo@GDY	Distal	*N_2+H^++e^-→*NNH	-0.36	Ma et al. 2021[17]
Rh SA/GDY	Enzymatic	*N_2+H^++e^-→*NNH	-0.44	Zou et al. 2021[18]
Pd-GDY	Distal	*N_2+H^++e^-→*NNH	-0.21	Yu et al. 2021[19]
Pt-3O structure	Distal	*N_2+H^++e^-→*NNH	-0.78	Hao et al. 2020[20]

References

1 J. K. Nørskov, J. Rossmeisl, A. Logadottir, et al. Origin of the overpotential for oxygen reduction at a fuel-cell cathode, Journal of Physical Chemistry B, 2004, 108, 17886-17892.

2 NIST Chemistry WebBook, https://webbook.nist.gov/chemistry/. accessed Feb 9, 2018.

3 Zhen Feng, Yanan Tang, Weiguang Chen, et al. Graphdiyne coordinated transition metals as single-atom catalysts for nitrogen fixation, Physical Chemistry Chemical Physical, 2020, 22, 9216-9224.

4 Zhigang Geng, Yan Liu, Xiangdong Kong, et al. Achieving a record-high yield rate of 120.9 μg NH_3 mg cat.$^{-1}$ h^{-1} for N_2 electrochemical reduction over Ru single-atom catalysts. Advanced Materials, 2018, 30(40), 1803498.

5 Xianghong Li, Tingshuai Li, Yongjun Ma, et al. Boosted electrocatalytic N_2 reduction to NH_3 by defect-rich MoS_2 nanoflower. Advanced Energy Materials, 2018, 8(30), 1801357.

6 Ling Zhang, Xuqiang Ji, Xiang Ren, et al. Electrochemical ammonia synthesis via nitrogen reduction reaction on a MoS_2 catalyst: Theoretical and experimental studies. Advanced Materials, 2018, 30(28), 1800191.

7 Xiang Ren, Jinxiu Zhao, Qin Wei, et al. High-performance N_2-to-NH_3 conversion electrocatalyzed by Mo_2C nanorod. ACS Central Science, 2019, 5(1), 116-121.

8 Hui Cheng, Liang-Xin Ding, Gao-Feng Chen, et al. Molybdenum carbide nanodots enable efficient electrocatalytic nitrogen fixation under ambient conditions. Advanced Materials, 2018, 30(46), 1803694.

9 Egill Skúlason, Bligaard Thomas, Gudmundsdóttir Sigrídur, et al. A theoretical evaluation of possible transition metal electro-catalysts for N_2 reduction. Physical Chemistry Chemical Physics, 2012, 14(3), 1235-1245.

10 Dongwei Ma, Zaiping Zeng, Liangliang Liu, et al. Computational evaluation of electrocatalytic nitrogen reduction on TM single-, double-, and triple-atom catalysts

(TM = Mn, Fe, Co, Ni) based on graphdiyne monolayers. The Journal of Physical Chemistry C, 2019, 123(31), 19066-19076.

11 Jingrui Han, Zaichun Liu, Yongjun Ma, et al. Ambient N_2 fixation to NH_3 at ambient conditions: Using Nb_2O_5 nanofiber as a high-performance electrocatalyst. Nano Energy, 2018, 52, 52264-270.

12 Yongyong Cao, Yijing Gao, Hu Zhou, et al. Highly efficient ammonia synthesis electrocatalyst: Single Ru atom on naturally nanoporous carbon materials. Advanced Theory and Simulations, 2018, 18000181-10.

13 Jingxiang Zhao, Zhongfang Chen. Single Mo atom supported on defective boron nitride monolayer as an efficient electrocatalyst for nitrogen fixation: A computational study. Journal of the American Chemical Society, 2017, 139(36), 12480-12487.

14 Huan Niu, Xiting Wang, Chen Shao, et al. Computational Screening Single-Atom Catalysts Supported on *g*-CN for N_2 Reduction: High Activity and Selectivity, ACS Sustainable Chemistry & Engineering, 2020, 8, 13749-13758.

15 Lan Hui, Yurui Xue, Huidi Yu, et al. Highly efficient and selective generation of ammonia and hydrogen on a graphdiyne-based catalyst. Journal of the American Chemical Society, 2019, 141(27), 10677-10683.

16 Cong Fang, Wei An. Single-metal-atom site with high-spin state embedded in defective BN nanosheet promotes electrocatalytic nitrogen reduction, Nano Research, 2021, 14, 4211-4219.

17 Dongwei Ma, Zaiping Zeng, Liangliang Liu, et al. Theoretical screening of the transition metal heteronuclear dimer anchored graphdiyne for electrocatalytic nitrogen reduction, Journal of Energy Chemistry, 2021, 54, 501-509.

18 Haiyuan Zou, Weifeng Rong, Shuting Wei, et al. Regulating kinetics and thermodynamics of electrochemical nitrogen reduction with metal single-atom catalysts in a pressurized electrolyser, PNAS, 2020, 117 (47), 29462-29468.

19 Huidi Yu, Yurui Xue, Lan Hui, et al. Graphdiyne-based metal atomic catalysts for synthesizing ammonia, National Science Review, 2021, 8(8), nwaa213.

20 Ran Hao, Wenming Sun, Qian Liu, et al. Efficient Electrochemical Nitrogen Fixation over Isolated Pt Sites, Small, 2020, 2000015.